Archives of Advances in Biosciences

Original Article

OPEN ACCESS

The Effect of Nettle (Urtica dioica) Extract and Its Green-Synthesized Silver Nanoparticles on the Growth and Biofilm Formation of Streptococcus mutans

Fa'ezeh Amiri rad[1], Simin Nabizadeh[2]*, Zahra Shafiei[3]

[1.] Faculty of Agriculture, Islamic Azad University, Roudehen Branch, Roudehen, Iran.
[2.] Faculty Member, Ph.D. in Plant Cellular and Developmental Biology, Department of Biology, Faculty of Agriculture, Islamic Azad University, Roudehen Branch, Roudehen, Iran. Email: Nabizadeh.simin@gmail.com
[3.]Department of Biology, Faculty of Agriculture, Islamic Azad University, Roudehen Branch, Roudehen, Iran.

Received: 01 Jan 2026; **Accepted:** 14 Jun 2026; **Published:** 15 Jun 2026

Cite this article as: Amiri rad F, Nabizadeh S, Shafiei Z. Antibacterial and Anti-Biofilm Activities of Urtica dioica aqueous extract and Greenly Synthesized Silver Nanoparticles Against Streptococcus mutans Archives of Advances in Biosciences. 2026 17(1):1-11. https://doi.org/10.22037/aab.v17i1.51429

Abstract

Background and Aim: The green biological synthesis of nanomaterials has attracted increasing attention due to its environmentally friendly nature and potential biomedical applications. This study aimed to comparatively evaluate the antibacterial and antibiofilm activities of aqueous *Urtica dioica* extract, its biosynthesized silver nanoparticles (AgNPs), and chlorhexidine against *Streptococcus mutans* PTCC 1683.

Methods: Silver nanoparticles were synthesized by adding aqueous *U. dioica* extract to a silver nitrate solution under controlled conditions. Key synthesis parameters, including extract volume, silver nitrate concentration, pH, and reaction time, were optimized to obtain stable nanoparticle formation. The resulting nanoparticles were characterized using UV–visible spectroscopy, FTIR, XRD, and SEM. Antimicrobial activity was assessed using agar well diffusion assay, while minimum inhibitory concentration (MIC) and minimum bactericidal concentration (MBC) were determined using standard broth dilution methods.

Results: Optimal synthesis conditions were achieved under neutral pH using 2 mL of plant extract and 4 mM silver nitrate. Characterization confirmed the formation of predominantly spherical nanoparticles with sizes in the range of 200–300 nm. In antibacterial assays, *U. dioica* aqueous extract showed the smallest inhibition zones, whereas AgNPs and chlorhexidine exhibited significantly stronger antibacterial activity. In biofilm assays, the aqueous extract demonstrated the lowest optical density (OD), indicating the strongest antibiofilm effect, while AgNPs and chlorhexidine showed comparable inhibitory effects on biofilm formation.

Conclusion: These findings suggest that *Urtica dioica* aqueous extract and its green-synthesized silver nanoparticles may serve as promising natural candidates for oral-care applications aimed at controlling *S. mutans* and dental caries. The results highlight their potential as alternative antimicrobial agents for biomedical and dental applications.

Keywords: Biofilm; Green synthesis; Silver nanoparticles; *Urtica dioica*; *Streptococcus mutans.*

1. Introduction

Metallic nanoparticles represent an important class of nanostructured materials due to their distinctive physicochemical and biological properties. However, conventional physical and chemical synthesis techniques commonly involve hazardous reagents and harsh conditions, raising concerns regarding environmental safety and sustainability (1) Consequently, the development of environmentally friendly and sustainable alternatives for nanoparticle production has become a critical research priority. Biologically driven synthesis approaches have emerged as viable substitutes for traditional methods.

A wide range of biological systems, including fungi, bacteria, viruses, and higher plants, have been employed for the fabrication of metal nanoparticles through low-cost and energy-efficient processes. These approaches, generally referred to as green synthesis, are attractive due to their operational simplicity, environmental compatibility, and capacity to generate stable nanoparticles with well-defined sizes and morphologies (2). Among biological sources, plant-based systems have gained particular attention as renewable and scalable platforms for nanoparticle synthesis. In contrast to microbial routes—which require strict culture conditions and may increase production costs—plant-mediated synthesis offers a more practical and economical alternative (3). Numerous plant species, including camphor, nettle, alfalfa, geranium, Eucalyptus spp., bitter olive, tamarind, gooseberry, Aloe vera, and coriander, have been successfully utilized for the extracellular biosynthesis of metallic nanoparticles. The effectiveness of plant extracts in nanoparticle synthesis is largely attributed to the presence of diverse bioactive constituents, such as secondary metabolites, proteins, enzymes, and other reducing or electron-donating compounds. These molecules facilitate the reduction of metal ions and contribute to nanoparticle stabilization. Silver nanoparticles (AgNPs) can be produced via physical, chemical, or biological routes (4,5); however, nanoscale silver exhibits enhanced reactivity and bioactivity as a result of its high surface-to-volume ratio and reduced particle size (6). Owing to these properties, AgNPs have been extensively investigated for applications in antimicrobial, antifungal, antiviral, anti-inflammatory, and anticancer fields (7). *Urtica dioica* (nettle) is one of the medicinal plants reported to be effective in the green synthesis of silver nanoparticles. This plant has a long history of use in traditional Iranian medicine for the management of conditions such as eczema, oral lesions, and various skin, gastrointestinal, and respiratory infections, with documented applications dating back to classical medical scholars including Galen and Avicenna. *Streptococcus mutans* is a Gram-positive, facultative anaerobic bacterium and a major component of the human oral microbiota. Approximately 25 species of oral streptococci have been identified, each occupying specific ecological niches within the oral cavity. Disruption of this microbial balance is closely associated with the development of oral and dental disorders. *S. mutans* plays a pivotal role in dental caries by fermenting dietary sucrose into lactic acid, leading to enamel demineralization, and by contributing to dental plaque formation through extracellular polysaccharide production (8). Considering the central role of *S. mutans* in dental caries and the reported antimicrobial potential of silver nanoparticles, the present study was designed to comparatively evaluate the effects of *U. dioica* aqueous extract and its green-synthesized silver nanoparticles on bacterial growth and biofilm formation of *S. mutans*.

2. Methods

Collection of Plant Material and Preparation of Aqueous Extract

Fresh *Urtica dioica* (nettle) plant material was collected from the surrounding areas of Tehran during the summer of 2021. Botanical identification and authentication of the plant material were performed in collaboration with the Herbarium and Plant Systematics Laboratory, Iran University of Medical Sciences. The collected samples were rinsed thoroughly with water to remove surface impurities and subsequently dried in an oven at 27 °C for three days. The dried plant material was then pulverized into a fine powder using an electric laboratory grinder (Waring, USA).

For aqueous extraction, 50 g of dried plant material (stems and leaves) was mixed with 500 mL distilled water preheated to 70–80 °C. The mixtures were sealed and incubated in a water bath at 60 °C for 24 h. Following incubation, the extracts were filtered using Whatman filter paper and a Büchner funnel to obtain clear aqueous solutions (9).

Green Synthesis of Silver Nanoparticles

Silver nanoparticles were synthesized by adding 10 mL of the filtered *U. dioica* aqueous extract, prepared by extracting 50 g of dried powder in 500 mL of distilled water, to 90 mL of 1 mM $AgNO_3$ solution (Merck, Germany). The reaction mixture was maintained at ambient temperature under dark conditions for 24 h to allow the reduction of Ag^+ ions (10). A visible color transition from pale yellow to dark brown or black was considered suggesting relatively more favorable conditions for nanoparticle formation under the tested experimental setup (11). The resulting colloidal suspensions were centrifuged at 8000 rpm for 20 min to recover the nanoparticle-containing fraction. This step may also collect partially aggregated silver nanostructures; therefore, the recovered pellets were considered AgNP-containing material rather than exclusively isolated primary nanoparticles. The collected pellets were then dried at 70 °C for 5 h (12).

Optimization of Synthesis Parameters

Optimization of Extract Volume (SPR-Based) Using UV–Vis Spectroscopy

To assess the influence of plant extract volume on nanoparticle synthesis, varying volumes (1–4 mL) of *U. dioica* aqueous extract were combined with 4 mL of 1 mM $AgNO_3$ solution. The reaction mixtures were

diluted to a final volume of 50 mL with distilled water. UV–Vis absorption spectra were recorded in the range of 200–400 nm, and the extract volume yielding the most pronounced SPR band (highest/most characteristic absorbance and/or peak shape) was selected as the optimal condition (13-15).

Effect of Silver Nitrate Concentration

Different concentrations of $AgNO_3$ (0.5, 1, 2, and 4 mM) were prepared to evaluate their effect on nanoparticle formation. The optical density of the reaction mixtures was measured using UV-Vis spectroscopy (UV-1800, Shimadzu, Japan) (13) within the 200–400 nm wavelength range. The concentration yielding the most favorable spectral characteristics was selected as optimal (15, 16).

Effect of pH and Reaction Time

To investigate the effect of pH, reaction mixtures containing 2 mL of plant extract and 4 mL of 1 mM $AgNO_3$ were adjusted to pH values ranging from 5 to 10 using 0.1 M NaOH or 0.1 M HCl. Each mixture was diluted to a final volume of 50 mL. UV–Vis spectra were recorded between 200 and 800 nm to identify the pH conditions most favorable for nanoparticle synthesis. Under optimized conditions, the influence of reaction time was monitored by recording UV–Vis spectra at 10-minute intervals for up to 60 min following reaction initiation (16-19).

Characterization of Synthesized Silver Nanoparticles

Fourier-Transform Infrared (FTIR) Analysis

FTIR spectroscopy was employed to identify functional groups involved in the reduction and stabilization of silver nanoparticles. Dried nanoparticle samples and powdered plant extract were separately mixed with potassium bromide (KBr) and analyzed using a Thermo Nicolet AVATAR 370 FTIR spectrometer (20).

X-ray Diffraction (XRD) Analysis

X-ray diffraction was employed to confirm the successful synthesis of silver nanoparticles, determine the type of crystal lattice, and estimate the particle size. The synthesized silver nanoparticles were analyzed using an XRD instrument operating at 40 kV and 40 mA with a copper (Cu) anode (21).

Scanning Electron Microscopy (SEM) Analysis

For SEM analysis, the nanoparticle suspension was centrifuged to obtain a concentrated pellet. A small volume of the suspension was deposited onto the sample holder and allowed to air-dry prior to imaging. SEM observations were performed using a KYKY EM3200 scanning electron microscope (22)

Biofilm Formation and Antimicrobial Evaluation Against Streptococcus mutans

Evaluation of Biofilm Formation by *Streptococcus mutans*

The ability of *Streptococcus mutans* PTCC 1683 (Provided by Islamic Azad University, Pharmaceutical Sciences Branch) to form biofilms and the antibiofilm activity of the *Urtica dioica* extract, silver nanoparticles, and chlorhexidine mouthwash 0.2 % (commercially available as Hexodine, Donyaye Behdasht Co., Tehran, Iran) were evaluated using a modified microtiter plate assay. Assays were performed at the Microbiology Laboratory of the School of Pharmaceutical Sciences. Bacterial activation involved streaking *S. mutans* PTCC 1683 onto Brain Heart Infusion Agar (BHIA; Merck) plates and incubating at 37°C for 24 hours. Fresh 24-hour cultures were used to prepare bacterial suspensions for the assays.

For biofilm quantification, 96-well polystyrene microtiter plates were utilized. After inoculation and incubation at 37°C for 24 hours to allow biofilm formation, non-adherent bacteria were removed by gently washing the wells with sterile distilled water. The adherent biofilms were stained using a fixed concentration of crystal violet solution (0.1% w/v) for 15 minutes. Following staining, excess stain was removed, and the wells were air-dried. The bound crystal violet was then solubilized using 95% ethanol. The quantity of biofilm was determined by measuring the optical density (OD) of the solubilized crystal violet at 570 nm using a microplate reader. Negative control wells containing sterile medium without bacteria or treatment were processed identically to establish a baseline. The percentage of biofilm inhibition was calculated using the following formula (15):

$$Biofilm\ inhibition\ \% = (1 - \frac{OD_{\text{treatment}}}{OD_{Control}}) \times 100$$

where $OD_{treatment}$ is the absorbance of treated wells and $OD_{control}$ is the absorbance of untreated biofilm control wells.

Agar Well Diffusion Assay

The antimicrobial activity of the test compounds was further evaluated using the agar well diffusion method. Briefly, bacterial suspensions (0.5 McFarland) were spread on Mueller-Hinton agar plates. Wells (6 mm in diameter) were created in the agar and filled with 100 µL of the respective compounds at different concentrations. After 24 h of incubation at 37 °C, the diameter of the inhibition zones was measured (mm). All experiments were performed in triplicate (23).

Determination of MIC and MBC by Broth Macrodilution Method

The minimum inhibitory concentration (MIC) and minimum bactericidal concentration (MBC) of *Urtica dioica* aqueous extract, synthesized silver nanoparticles, and chlorhexidine against Streptococcus mutans were determined using the broth

macrodilution method according to CLSI guidelines with minor modifications. Serial two-fold dilutions of each test compound were prepared in sterile Mueller–Hinton broth supplemented with appropriate growth conditions for *S. mutans*. Bacterial suspensions were adjusted to 0.5 McFarland standard (approximately 1.5×10^8 CFU/mL) and further diluted to obtain the final inoculum concentration. Each tube contained broth medium, the test compound at the desired concentration, and bacterial inoculum. Positive control tubes contained broth medium with bacterial inoculum without antimicrobial agents, while negative control tubes contained broth medium only. Following incubation at 37 °C for 24 h, MIC values were determined as the lowest concentration showing no visible bacterial growth. For MBC determination, aliquots from tubes without visible turbidity were subcultured onto Mueller–Hinton agar plates and incubated at 37 °C for an additional 24 h. The lowest concentration showing no bacterial colony growth was recorded as the MBC value. All experiments were performed in triplicate (24,25).

Evaluation of the Effect of Silver Nanoparticles on Biofilm Formation

The effects of silver nanoparticles, chlorhexidine, and *U. dioica* aqueous extract on biofilm formation were evaluated using a microtiter plate assay. To identify the effects of silver nanoparticles, chlorhexidine, and plant extract on biofilm formation, 190 µL of Brain Heart Infusion (BHI) broth was added to the wells of a 96-well polystyrene microplate (SPL, South Korea) as follows:

Well 1: Medium without silver nanoparticles, chlorhexidine, or extract (positive control).

Well 2: Medium containing 0.5× MIC of silver nanoparticles, chlorhexidine, or extract.

Well 3: Medium containing 1× MIC of silver nanoparticles, chlorhexidine, or extract.

Well 4: Medium containing 2× MIC of silver nanoparticles, chlorhexidine, or extract.

Well 5: Medium without silver nanoparticles, chlorhexidine, extract, or bacterial suspension (negative control).

These conditions were applied separately for each treatment group, including plant extract, silver nanoparticle solution, and chlorhexidine. Subsequently, 10 µL of a freshly prepared bacterial suspension adjusted to a 0.5 McFarland standard was added to wells (i)–(iv), while sterile distilled water was added to the negative control wells. The plates were incubated at 37 °C for 24 h to allow biofilm development. After incubation, the contents of the wells were gently discarded, and each well was washed three times with distilled water to remove planktonic cells, leaving the adherent biofilm intact. Biofilms were then stained by adding 200 µL of 0.025% safranin solution to each well and incubating for 2 min. Excess stain was removed, and the wells were rinsed three times with distilled water. To solubilize the bound dye, 200 µL of a 1:1 ethanol–acetone solution was added to each well and incubated for 15 min. The optical density (OD) of the released stain was measured at 492 nm using a 96-well ELISA reader (Convergent, Germany). The negative control well was processed under identical conditions to the test wells, including the washing and staining steps. The mean OD value of the negative control (0.019±0.00) was subtracted from all experimental OD values to correct for non-specific background absorbance. All reported results represent these corrected values (26).

Statistical Analysis

All quantitative data were subjected to statistical analysis using one-way analysis of variance (ANOVA) within a completely randomized design framework. Data analysis was performed using SPSS software (version 20). All experiments were conducted in triplicate under randomized conditions. Differences among mean values were evaluated using Duncan's multiple range test, and statistical significance was defined at $P \leq 0.05$.

3. Results

Optimization of Parameters Affecting Silver Nanoparticle Synthesis

a) Effect of Extract Concentration

UV–visible spectrophotometric analysis revealed that silver nanoparticles synthesized in the presence of 2 mL of *U. dioica* aqueous extract exhibited the highest absorbance intensity, indicating more efficient nanoparticle formation compared with other tested volumes (Figure 1). As shown in Figure 1, the characteristic surface plasmon resonance peak was most pronounced at this extract concentration, confirming its selection as the optimal condition for subsequent experiments.

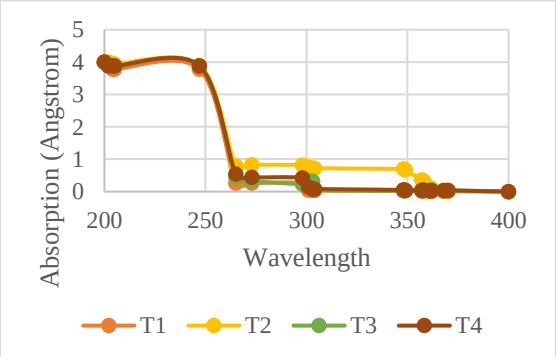

Figure 1. UV–Vis spectra of silver nanoparticles synthesized using different volumes of *Urtica dioica* aqueous extract (T1: 1 mL, T2: 2 mL, T3: 3 mL, T4: 4 mL).

Archives of Advances in Biosciences

b) Effect of Silver Nitrate Concentration on Nanoparticle Synthesis

The effect of varying silver nitrate ($AgNO_3$) concentrations on the synthesis of silver nanoparticles (AgNPs) was investigated across the 200–400 nm wavelength range using UV-Vis spectroscopy (Figure 2). Across all tested concentrations (T1: 0.5 mM, T2: 1 mM, T3: 2 mM, T4: 4 mM), the spectra exhibited a general decrease in absorbance as the wavelength increased. However, subtle concentration-dependent differences were observed. Specifically, the spectrum corresponding to 4 mM $AgNO_3$ (T4) showed a marginally higher overall absorbance and a slightly less abrupt decrease in absorption around the 300–320 nm region compared to lower concentrations. While no distinct Surface Plasmon Resonance (SPR) peak was clearly defined in this range, these spectral characteristics suggest that the 4 mM concentration facilitated a more efficient formation or stabilization of silver nanoparticles under the employed reaction conditions. Therefore, 4 mM silver nitrate was considered the optimal concentration for subsequent synthesis experiments. Representative SEM images of the nanoparticles synthesized at this concentration, in the presence of *U. dioica* aqueous extract, are shown in Figure 3.

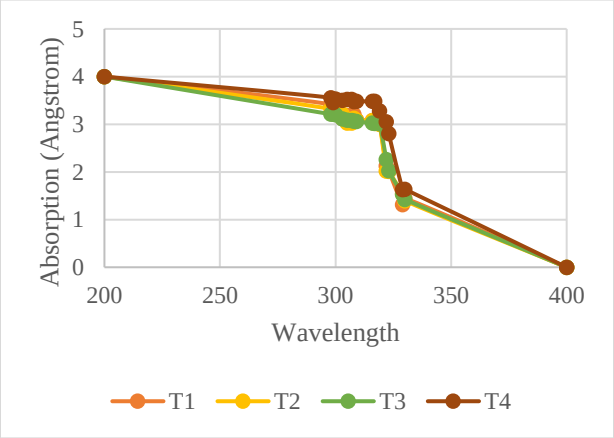

Figure 2. UV–Vis spectra of silver nanoparticles synthesized with different concentrations of silver nitrate (wavelength, nm) in the presence of 2 mL of Urtica dioica aqueous extract (T1: 0.5 mM, T2: 1 mM, T3: 2 mM, T4: 4 mM).

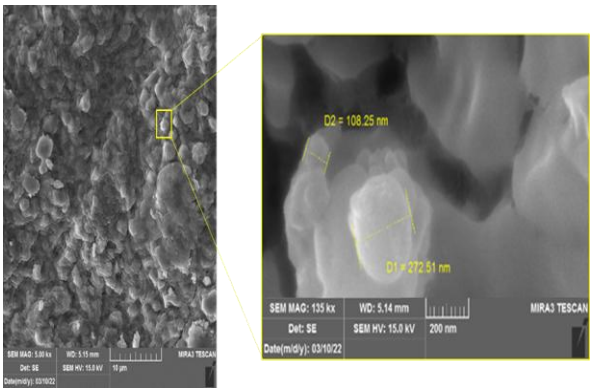

Figure 3. Transmission electron microscopy images of silver nanoparticles synthesized with *Urtica dioica* aqueous extract at the optimal concentration.

c) Effect of pH

Analysis of UV–Vis spectra indicated that increasing the pH of the reaction medium enhanced the surface plasmon resonance (SPR) absorbance of the synthesized silver nanoparticles (Figure 4). This increasing trend continued up to pH 7, beyond which no further enhancement in absorbance was observed. In contrast, reactions conducted at lower pH values exhibited a marked reduction in absorbance intensity. Statistical analysis revealed a significant difference in absorbance at 300 nm ($P \leq 0.05$), supporting the selection of neutral pH as the optimal condition for nanoparticle synthesis. Evaluation of reaction time showed no statistically significant effect on the absorbance of silver nanoparticles synthesized using *U. dioica* aqueous extract ($P > 0.05$), indicating that nanoparticle formation was not strongly time-dependent under the tested conditions.

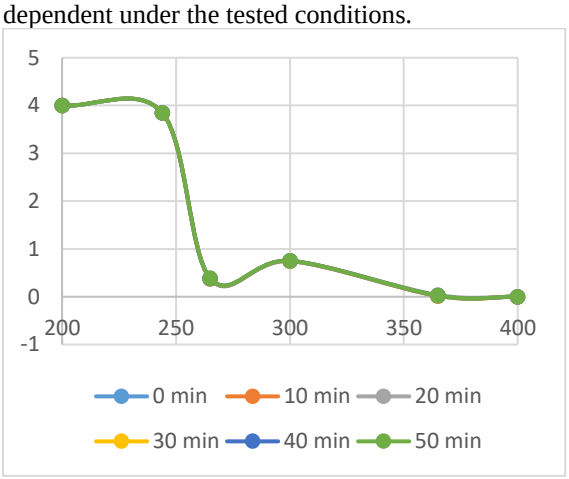

Figure 4. UV–Vis spectra of silver nanoparticle solutions synthesized at 25 °C under different pH conditions (wavelength, nm).

d) X-ray Diffraction (XRD) Analysis

The XRD pattern of the synthesized silver nanoparticles indicated broad peaks, reflecting the

small size of the nanoparticles. As the particle size decreases, the diffraction peaks broaden (Figure 5). The observed diffraction peaks at 2θ=38.07°, 44.26°, 64.43°, and 77.35° correspond to the (111), (200), (220), and (311) planes of face-centered cubic (FCC) silver nanoparticles, respectively.

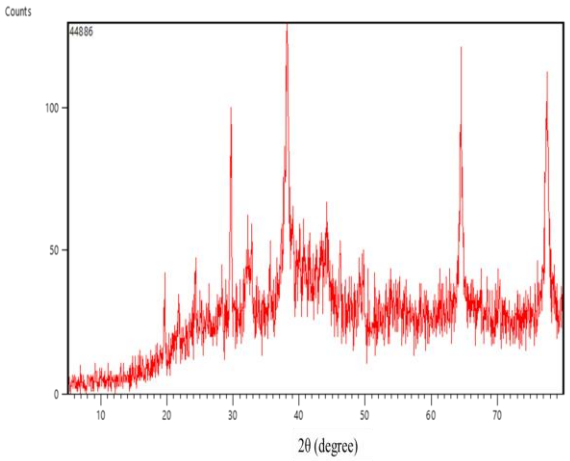

Figure 5. X-ray diffraction spectrum of synthesized nanoparticles

e) Fourier-Transform Infrared (FTIR) Analysis

The FTIR spectrum of silver nanoparticles synthesized with *Urtica dioica* extract at the optimal concentration is shown in Figure 6. The spectrum displayed peaks corresponding to vibrational modes at 4688, 3742, 3437, 2925, 2055, 1629, 1378, 1088, and 1040 cm^{-1}, indicating the presence of functional groups involved in the reduction and stabilization of silver nanoparticles.

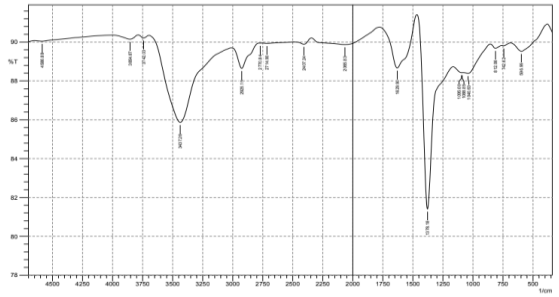

Figure 6. FTIR spectrum of silver nanoparticles synthesized using *Urtica dioica* aqueous extract at the optimal concentration.

Microbiological Results

a) MIC and MBC Evaluation

The minimum inhibitory concentration (MIC) and minimum bactericidal concentration (MBC) values of the tested agents are summarized in Table 1. Chlorhexidine exhibited both MIC and MBC values of 8 µg/mL. In comparison, silver nanoparticles synthesized using *U. dioica* aqueous extract showed a MIC of 4 µg/mL and an MBC of 5 µg/mL. The plant extract alone demonstrated lower antibacterial activity, with MIC and MBC values of 3 µg/mL.

Table 1. MIC and MBC values of different treatments against *Streptococcus mutans*.

Treatment	MIC (µg/mL)	MBC (µg/mL)
Urtica dioica aqueous extract	3	3
Chlorhexidine	8	8
Silver nanoparticles synthesized from *Urtica dioica* aqueous extract	4	5

b) Antibacterial activity by agar well diffusion assay

The antibacterial activities of *Urtica dioica* aqueous extract, silver nanoparticles synthesized with the extract, and chlorhexidine are presented in Table 2. *Streptococcus mutans* showed sensitivity to all three treatments at concentrations of 0.5, 1, and 2 µg/mL. The smallest inhibition zones were observed for the plant extract, whereas the largest inhibition zones were recorded for silver nanoparticles and chlorhexidine. Statistical analysis confirmed that these differences were significant ($P \leq 0.05$).

Table 2. Mean diameter (mm) of inhibition zones of Streptococcus mutans treated with Urtica dioica aqueous extract, silver nanoparticles, and chlorhexidine at different concentrations (µg/mL).

Treatment	0.5	1	2
***Urtica dioica* aqueous extract**	3.00 ± 1.00[a]	9.66 ± 0.57[b]	9.66 ± 0.57[b]
Silver nanoparticles synthesized from *Urtica dioica* aqueous extract	5.33 ± 1.52[a]	12.00 ± 2.00[b]	12.66 ± 2.08[b]
Chlorhexidine	4.00 ± 2.00[a]	14.00 ± 1.00[b]	14.33 ± 0.57[b]

Means in each column labeled with different letters indicate statistically significant differences (P<0.05).

c) Biofilm Formation by *Streptococcus mutans*

The antibiofilm activity of the *Urtica dioica* extract, synthesized silver nanoparticles, and chlorhexidine against *Streptococcus mutans* was assessed using a microtiter plate assay. As shown in Table 3, all tested agents demonstrated a significant ability to inhibit biofilm formation compared to the positive control.

The positive control wells, containing bacteria without any inhibitory agents, showed the highest optical density (OD) at 492 nm (0.35 ± 0.00), indicating robust biofilm formation under the experimental conditions. In contrast, the negative control wells, which contained only sterile medium without bacteria, exhibited a minimal OD (0.019 ± 0.00), confirming the

specificity of the assay and the absence of significant background staining.

The *Urtica dioica* extract demonstrated the strongest antibiofilm activity, resulting in the lowest OD value among the treatment groups (0.115 ± 0.00). Silver nanoparticles synthesized using the *Urtica dioica* extract and chlorhexidine showed comparable efficacy, both yielding OD values of approximately 0.220-0.222 (0.220 ± 0.005 and 0.222 ± 0.00, respectively).

Statistical analysis revealed significant differences between the groups ($p < 0.05$). The OD values were grouped into distinct statistical categories denoted by superscript letters: 'a' for the negative control, 'b' for the positive control, 'c' for the *Urtica dioica* extract, and 'd' for both silver nanoparticles and chlorhexidine. This grouping indicates that the *Urtica dioica* extract was significantly more effective in inhibiting biofilm formation than both silver nanoparticles and chlorhexidine, while silver nanoparticles and chlorhexidine exhibited similar levels of antibiofilm activity, both significantly outperforming the positive control.

Table 3. Optical density (OD) of *Streptococcus mutans* biofilm formation in the presence of extract, chlorhexidine, and extract-mediated silver nanoparticles

Treatments	Mean ± SD (MIC 0.5)
Extract	0.115 ± 0.00^{c}
Chlorhexidine	0.222 ± 0.00^{d}
Silver nanoparticles synthesized using *Urtica dioica* aqueous extract	0.220 ± 0.005^{d}
Positive control	0.35 ± 0.00^{b}
Negative control	0.019 ± 0.00^{a}

Means followed by different letters in each column are significantly different ($P<0.05$).

4. Discussion

The global increase in bacterial infections, coupled with rising antibiotic resistance, has driven interest in nanotechnology-based antimicrobial strategies (27). Among these, silver nanoparticles (AgNPs) exhibit strong antibacterial activity, largely due to their high surface-to-volume ratio. AgNPs have been shown to be effective against both Gram-positive and Gram-negative bacteria, as well as molds and fungi, making them a promising alternative to conventional antimicrobial agents .

Silver can be converted into nanoparticles via various physical, chemical, and biological approaches, including chemical reduction, sonochemistry, irradiation, and green (bio-based) synthesis (28,29). In green synthesis, plant-derived compounds act as reducing agents, enabling the conversion of metal ions into nanoparticles without the need for surfactants, extreme conditions, or additional stabilizers. Bioactive and water-soluble metabolites in plant extracts facilitate this process at ambient temperature (14).

In this study, AgNPs were synthesized using *Urtica dioica* aqueous extract, and their antibacterial properties were evaluated. UV–Vis analysis suggested that increasing the extract concentration promoted nanoparticle formation, as reflected by higher absorbance values. This observation is consistent with previous reports showing that plant extract volume can influence the rate and extent of nanoparticle synthesis (15).

The extract, rich in antioxidant compounds (24), likely acted as both a reducing and stabilizing agent. The highest absorbance was observed at 2 mL of extract, suggesting that increasing the extract volume from 1 to 2 mL improved the reduction of Ag^{+} ions and favored nanoparticle formation. At 4 mL, however, absorbance did not increase further, which may indicate that an excess of extract altered the capping environment and affected nanoparticle stabilization. Thus, 2 mL appeared to provide the most suitable balance between reduction and stabilization under the present conditions (31,32).

Likewise, increasing the silver nitrate concentration influenced the UV–Vis spectral profile of the synthesized nanoparticles. Among the tested concentrations, 4 mM showed the most favorable overall absorbance behavior within the 200–400 nm range, suggesting enhanced availability of Ag^{+} ions for reduction and nanoparticle formation. Since no distinct SPR peak was observed in this range, the interpretation is based on the general spectral trend rather than a specific resonance maximum. Similar precursor-dependent effects have been reported in previous studies (15).

pH is one of the most critical factors influencing nanoparticle synthesis (16) Previous studies have reported that pH affects both the formation and stability of nanoparticles. In the present study, increasing the reaction pH enhanced the surface plasmon resonance absorbance of silver nanoparticles. This may be attributed to changes in the ionization state of biomolecules in the extract, which can affect reduction efficiency and capping/stabilization behavior (17–19,33).

XRD analysis confirmed the formation of crystalline silver nanostructures, with peaks at $2\theta = 38.07°$ (111),

44.26° (200), 64.43° (220), and 77.35° (311), corresponding to the FCC structure of silver, consistent with standard XRD patterns and previous reports (14, 29, 34–36).

Proteins appear to play a key role in nanoparticle formation and stabilization. Free amino groups and other biomolecular functional groups may bind to the nanoparticle surface, enhancing stability. FTIR analysis further supported the presence of biomolecules acting as capping agents that contribute to nanoparticle stabilization. In this study, FTIR spectra recorded over the 500–4500 cm^{-1} range revealed characteristic peaks at 3742, 3437, 2925, 2055, 1629, 1378, 1088, 1040, and 4688 cm^{-1}, corresponding to functional groups involved in silver ion reduction.

FTIR analysis revealed broad absorption bands in the 3437–4688 cm^{-1} range, corresponding to O–H stretching vibrations of alcohols, phenols, and carboxylic acids, as well as N–H stretching in amides and amines. A band near 2055 cm^{-1} indicated secondary amine (N–H) stretching and C–H vibrations in alkynes and aldehydes. Peaks between 1629 and 2925 cm^{-1} were assigned to C=O, C=C, and C=N stretching modes from aldehydes, alkenes, esters, acetic acids, proteins, amino acids, and aromatic rings present in the plant extract. Absorption bands in the 1040–1378 cm^{-1} range reflected alcohols, ethers, carboxyl, phosphate groups, and aliphatic proteins or amines. Biomolecules such as carbonyl compounds, flavonoids, tannins, and other phenolics likely contributed to the reduction of silver ions and the stabilization of nanoparticles. The UV–Vis spectra confirmed enhanced localized surface plasmon resonance (LSPR), which is characteristic of metallic nanoparticles. According to Mie theory, spherical silver nanoparticles exhibit a single plasmon band, while anisotropic particles may show multiple bands (37, 38).

The microbiological results of the present study showed that the antibacterial and antibiofilm activities of the tested agents varied depending on the assay used. In the MIC and MBC evaluations, the silver nanoparticles synthesized using *Urtica dioica* extract exhibited stronger antibacterial activity than the aqueous plant extract, while chlorhexidine remained an effective comparative antimicrobial agent. Similarly, in the well diffusion assay, the nanoparticles produced larger inhibition zones than the plant extract, suggesting superior diffusion-related antibacterial performance under the tested conditions (26,38,39). These findings are in agreement with previous studies reporting that silver nanoparticles exert antibacterial effects through multiple mechanisms, including disruption of membrane integrity, interaction with sulfhydryl- and phosphate-containing cellular components, and induction of reactive oxygen species (19,39,40).

In contrast, the biofilm assay demonstrated a different pattern, as the aqueous *U. dioica* aqueous extract produced the lowest OD value and therefore the strongest inhibition of biofilm formation against *Streptococcus mutans*. The synthesized silver nanoparticles also inhibited biofilm formation, but their effect was less pronounced than that of the extract. This difference may be explained by the distinct requirements of planktonic growth inhibition and biofilm suppression. Biofilm formation is a complex process involving bacterial adhesion, extracellular polymeric substance production, quorum sensing, and maturation of the biofilm matrix (41–44). Plant extracts rich in phenolic compounds and flavonoids have been reported to interfere with these processes by inhibiting adhesion, reducing extracellular matrix production, and modulating quorum sensing pathways (41–44). Therefore, the stronger antibiofilm effect of the *U. dioica* aqueous extract in the present study may be related to its phytochemical composition and its ability to interfere with early biofilm development steps.

It should be emphasized that no formal synergistic test was performed between the *U. dioica* aqueous extract and the synthesized silver nanoparticles in the current study. Accordingly, no conclusion regarding synergy can be made. Instead, the results indicate that the relative efficacy of the tested agents depends on the specific endpoint being evaluated. While silver nanoparticles were more effective in the MIC/MBC and well diffusion assays, the aqueous plant extract showed superior antibiofilm activity in the crystal violet assay. Such assay-dependent differences have been reported in previous studies and should be interpreted accordingly (39–44).

5. Conclusion

The present findings indicate that the aqueous *Urtica dioica* extract and its green-synthesized silver nanoparticles exhibit distinct antibacterial and antibiofilm activities against *Streptococcus mutans*. While both AgNPs and chlorhexidine demonstrated strong antibacterial efficacy, the aqueous *Urtica dioica* extract exhibited the most potent antibiofilm effect. These results highlight the potential of both the extract and its biosynthesized AgNPs as promising natural agents for controlling *S. mutans* and preventing dental caries, warranting further investigation for development in oral-care formulations.

Acknowledgments

The authors would like to express their sincere gratitude to the Department of Biology and the Research Deputy of Islamic Azad University,

Roudehen Branch, for their valuable technical and administrative support throughout this study.

Ethical Considerations and Compliance with Ethical Guidelines

This study was conducted in vitro using standard laboratory strains of Streptococcus mutans. As this research involved no human or animal participants, ethical approval from an Institutional Review Board (IRB) or an Ethics Committee was not required. The study strictly adhered to biosafety and laboratory safety guidelines for handling microorganisms. Furthermore, no conflict of interest is declared by the authors.

Funding

This research received no external funding.

Conflict of interest

There is no conflict of interest.

AI Using Declaration

During the preparation of this manuscript, the authors used DeepSeek-V3 (accessed on May 3, 2026) solely for the purpose of final language editing, grammatical refinement, and checking for potential unintentional plagiarism.The tool was not used to generate research data, analyze results, or draw scientific conclusions. The authors have reviewed and edited the final output and take full responsibility for the content of the manuscript.

Author's contributions

Conception and design: Fa'ezeh Amiri, Simin Nabizadeh, Zahra Shafiei.
Provision of study materials and reagents: Fa'ezeh Amiri, Simin Nabizadeh, Zahra Shafiei.
Collection and assembly of data: Fa'ezeh Amiri, Simin Nabizadeh, Zahra Shafiei.
Data analysis and interpretation: Fa'ezeh Amiri, Simin Nabizadeh, Zahra Shafiei.
Manuscript writing: Fa'ezeh Amiri.
Final approval of manuscript: All authors.

6. References

1. Ashrafi G, Nasrollahzadeh M, Jaleh B, Sajjadi M, Ghafuri H. Biowaste-and nature-derived (nano) materials: Biosynthesis, stability and environmental applications. Advances in Colloid and Interface Science. 2022 Mar;301:102599. (DOI: 10.1016/j.cis.2022.102599) (PMID)

2. Abbar JC, Swetha G, Meti MD, Byadagi KS. Environmental applications of green engineered silver nanoparticles. In: Phytonanotechnology. Springer Nature Singapore; 2022, p. 199-225. (DOI: 10.1007/978-981-19-4811-4_10)

3. Chandran SP, Chaudhary M, Pasricha R, Ahmad A, Sastry M. Synthesis of gold nanotriangles and silver nanoparticles using Aloevera plant extract. Biotechnology progress. 2006 Mar-Apr;22(2):577-83. (DOI: 10.1021/bp0501423) (PMID)

4. Baghizadeh A, Ranjbar S, Gupta VK, Asif M, Pourseyedi S, Karimi MJ, et al. Green synthesis of silver nanoparticles using seed extract of Calendula officinalis in liquid phase. Journal of Molecular Liquids. 2015 Mar;207:159-63. (DOI: 10.1016/j.molliq.2015.03.029)

5. Firdhouse MJ, Lalitha P. Biogenic green synthesis of gold nanoparticles and their applications – A review of promising properties. Inorganic Chemistry Communications. 2022 Sep;143:109800. (DOI: 10.1016/j.inoche.2022.109800)

6. Shankar SS, Rai A, Ahmad A, Sastry M. Rapid synthesis of Au, Ag, and bimetallic Au core– Ag shell nanoparticles using Neem (Azadirachta indica) leaf broth. Journal of Colloid and Interface Science. 2004 Jul;275(2):496-502. (DOI: 10.1016/j.jcis.2004.03.003) (PMID)

7. Sakthi Devi R, Girigoswami A, Siddharth M, Girigoswami K. Applications of gold and silver nanoparticles in theranostics. Applied Biochemistry and Biotechnology. 2022 Sep;194(9):4187-219. (DOI: 10.1007/s12010-022-03963-z) (PMID)

8. Chathoth KN. Effect of environmental signals on the development of oral biofilm. Ph.D. Thesis. Université Rennes 1; 2021. (LINK)

9. United Nations Industrial Development Organization, Handa, S. S., Khanuja, S. P. S., Longo, G., & Rakesh, D. D. (2008). Extraction technologies for medicinal and aromatic plants. Earth, environmental and marine sciences and technologies.(LINK)

10.Jacob SJP, Finub J, Narayanan A. Synthesis of silver nanoparticles using Piper longum leaf extracts and its cytotoxic activity against Hep-2 cell line. Colloids and Surfaces, B: Biointerfaces. 2012 Mar;91:212-4. (DOI: 10.1016/j.colsurfb.2011.11.001) (PMID)

11.Khane Y, Benouis K, Albukhaty S, Sulaiman GM, Abomughaid MM, Al Ali A, et al. Green synthesis of silver nanoparticles using aqueous *Citrus limon* zest extract: Characterization and evaluation of their antioxidant and antimicrobial properties. Nanomaterials. 2022 Jun;12(12):2013. (DOI: 10.3390/nano12122013) (PMID)

12.Ajitha B, Reddy YAK, Reddy PS. Green synthesis and characterization of silver nanoparticles using Lantana camara leaf extract. Materials Science and Engineering: C. 2015 Apr;49:373-81. (DOI: 10.1016/j.msec.2015.01.035) (PMID)

13.Suresh G, Gunasekar PH, Kokila D, Prabhu D, Dinesh D, Ravichandran N, et al. Green synthesis of silver nanoparticles using Delphinium denudatum root extract exhibits antibacterial and mosquito larvicidal activities.

Spectrochimica Acta Part A: Molecular and Biomolecular Spectroscopy. 2014 Feb;127:61-6. (DOI:10.1016/j.saa.2014.02.030)
14.Mittal AK, Chisti Y, Banerjee UC. Synthesis of metallic nanoparticles using plant extracts. Biotechnology Advances. 2013 Mar;31(2):346-56. (DOI:10.1016/j.biotechadv.2013.01.003
15.Dwivedi AD, Gopal K. Biosynthesis of silver and gold nanoparticles using Chenopodium album leaf extract. Colloids and Surfaces A: Physicochemical and Engineering Aspects. 2010 Oct;369(1-3):27-33. (DOI: 10.1016/j.colsurfa.2010.07.020)
16.Waghmare SS, Deshmukh AM, Sadowski Z. Biosynthesis, optimization, purification and characterization of gold nanoparticles. African Journal of Microbiology Research. 2014 Jan;8(2):138-46. (DOI: 10.5897/AJMR10.143)
17.Gardea-Torresdey J, Tiemann K, Gamez G ,Dokken K, Tehuacanero S, Jose-Yacaman M. Gold nanoparticles obtained by bio-precipitation from gold (III) solutions. Journal of Nanoparticle Research. 1999;1:397-404. (DOI: 10.1023/A:1010008915465)
18. Armendariz V, Herrera I, Peralta-Videa JR, Jose-Yacaman M, Troiani H, Santiago P, et al. Size controlled gold nanoparticle formation by Avena sativa biomass: use of plants in nanobiotechnology. Journal of Nanoparticle Research. 2004 Aug;6(4):377-82. (DOI: 10.1007/s11051-004-0741-4)
19.Mironov I, Makotchenko E. The hydrolysis of AuCl 4− and the stability of aquachlorohydroxocomplexes of gold (III) in aqueous solution. Journal of Solution Chemistry. 2009 June;38(6):725-37. (DOI:10.1007/s10953-009-9400-9)

20.Nikparast Y, Ghorbani R, Ahmadzadeh H, Asadi G. Green synthesis of silver nanoparticles using Amarantus retroflexus and its antibacterial effect. 2018. (LINK)

21.Dousti B, Nabipour F, Hajiamraei A. Green synthesis of silver nanoparticle by using the aqueous extract of Fumaria Parviflora and investigation of their antibacterial and antioxidant activities. Razi Journal of Medical Sciences. 2019;26(6):105-17. (LINK)

22.Pirtarighat S, Ghannadnia M, Baghshahi S. Green synthesis of silver nanoparticles using the plant extract of Salvia spinosa grown in vitro and their antibacterial activity assessment. Journal of Nanostructure in Chemistry. 2019;9:1-9.(Doi:10.1007/s40097-018-0291-4)
23.Nwuche, C. O., Ujam, O. T., Ibezim, A., & Ujam, I. B. (2017). Experimental and in-silico investigation of anti-microbial activity of 1-chloro-2-isocyanatoethane derivatives of thiomorpholine, piperazine and morpholine. *Plos one*, *12*(1). DOI: 10.1371/journal.pone.0170150

24.Moradi P, Amini K. Extraction and identification of *Urtica dioica* L extract and its antibacterial and antifungal properties. Journal of Mazandaran University of Medical Sciences. 2017;27(151):74-85. (LINK)
25.McFarland J. The nephelometer: an instrument for estimating the number of bacteria in suspensions used for calculating the opsonic index and for vaccines. Journal of the American Medical Association. 1907;XLIX(14):1176-8. (DOI:10.1001/jama.1907.25320140022001f)

26.Stepanović, S., Vuković, D., Dakić, I., Savić, B., & Švabić-Vlahović, M. (2000). A modified microtiter-plate test for quantification of staphylococcal biofilm formation. Journal of microbiological methods, 40(2), 175-179. (DOI: 10.1016/S0167-7012(00)00122-6)

27.Rezaei-Zarchi S, Javed A, Ghani MJ, Soufian S, Barzegari FF, Bayaduri MA, et al. Comparative study of antimicrobial activities of TiO2 and CdO nanoparticles against the pathogenic strain of Escherichia coli. Iranian Journal of Pathology. 2010;5(2):83-9. (LINK)
28.Owen EA, Williams GI. A low-temperature X-ray camera. Journal of Scientific Instruments. 1954;31(2):49. (DOI 10.1088/0950-7671/31/2/305)
29.Penalver P, Huerta B, Borge C, Astorga R, Romero R, Perea A. Antimicrobial activity of five essential oils against origin strains of the Enterobacteriaceae family. APMIS: Acta Pathologica, Microbiologica, et Immunologica Scandinavica. 2005 Jan;113(1):1-6. (DOI: 10.1111/j.1600-0463.2005.apm1130101.x) (PMID)
30.Bhusal KK, Magar SK, Thapa R, Lamsal A, Bhandari S, Maharjan R, et al. Nutritional and pharmacological importance of stinging nettle (*Urtica dioica* L.): A review. Heliyon. 2022 Jun;8(6):e09717. (DOI: 10.1016/j.heliyon.2022.e09717) (PMID)
31.Bano F, Baber M, Ali A, Shah Z, Muhammad SA. Biosynthesis, characterization, and biological activities of iron nanoparticles using Sesamum indicum seeds extract. Pharmacognosy Magazine. 2017 Apr;13(49):33-6. (DOI: 10.4103/0973-1296.203985)
32.Foroughi Rad S, Khatibzadeh M. Green synthesis of silver nano particles for conductive inks, using sonochemical technique. Nashrieh Shimi va Mohandesi Shimi Iran. 2015;34(1):1-9. (LINK)
33.Subhani MA, Irshad M, Nazir A, Hafeez M, Ali S. Synthesis and antibacterial potential of Loranthus pulverulentus conjugated silver nanoparticles. Microscopy Research and Technique. 2022 Nov;85(11):3530-40. (DOI: 10.1002/jemt.24204) (PMID)
34.Krishnaraj C, Jagan E, Rajasekar S, Selvakumar P, Kalaichelvan P, Mohan N. Synthesis of silver nanoparticles using Acalypha indica leaf extracts and its antibacterial activity against water borne pathogens. Colloids and

Archives of Advances in Biosciences

Surfaces B: Biointerfaces. 2010 Mar;76(1):50-6. (DOI: 10.1016/j.colsurfb.2009.10.008) (PMID)

35.Singh PK, Bhardwaj K, Dubey P, Prabhune A. UV-assisted size sampling and antibacterial screening of Lantana camara leaf extract synthesized silver nanoparticles. RSC Advances. 2015 Feb;5(31):24513-20. (DOI:10.1039/C4RA17233G)

36.Sökmen M, Serkedjieva J, Daferera D, Gulluce M, Polissiou M, Tepe B, et al. In vitro antioxidant, antimicrobial, and antiviral activities of the essential oil and various extracts from herbal parts and callus cultures of Origanum acutidens. Journal of Agricultural and Food Chemistry. 2004 Jun;52(11):3309-12. (DOI: 10.1021/jf049859g) (PMID)

37.Khlebtsov NG, Dykman LA, Khlebtsov BN. Synthesis and plasmonic tuning of gold and gold±silver nanoparticles. Russian Chemical Reviews. 2022 Nov;91(10):RCR5058. (DOI:10.57634/RCR5058)

38.Nikoobakht B, Wang J, El-Sayed MA. Surface-enhanced Raman scattering of molecules adsorbed on gold nanorods: off-surface plasmon resonance condition. Chemical Physics Letters. 2002 Nov;366(1-2):17-23. (DOI:10.1016/S0009-2614(02)01492-6)

39.Panyala NR, Peña-Méndez EM, Havel J. Silver or silver nanoparticles: a hazardous threat to the environment and human health? Journal of applied biomedicine. 2008;6(3).(LINK)

40.Virk K, Sharma K, Kapil S, Kumar V, Sharma V, Pandey S, et al. Synthesis of gum acacia-silver nanoparticles based hydrogel composites and their comparative anti-bacterial activity. Journal of Polymer Research. 2022 Apr;29(4):118. (DOI:10.1007/s10965-022-02978-8)

41.Hosseini F, Ghavam Shirazi M, Norouzi J. The effects of antimicrobial agents on planktonic and biofilm strains of streptococcus mutans isolated from dental plague. Internal Medicine Today. 2011;17(2):5-13. (LINK)

42.Ranjbar F, Eslami G, Ghahremanloo A, Taheri S, Ayatollahi M, Eslami S. Antibacterial effect of green tea extract on Streptococcus mutans and Enterococcus faecalis isolated from dental plaque. Journal of Mashhad Dental School. 2016 Jan;39(4):335-42. (DOI: 10.22038/jmds.2015.5807)

43.Neturi RS, Srinivas R, Kumar S. Effects of green tea on Streptococcus mutans counts-a randomised control trail. Journal of Clinical and Diagnostic Research: JCDR. 2014 Nov;8(11):ZC128-30. (DOI: 10.7860/JCDR/2014/10963.5211) (PMID)

44.Thomas A, Thakur SR, Shetty SB. Anti-microbial efficacy of green tea and chlorhexidine mouth rinses against Streptococcus mutans, Lactobacilli spp. and Candida albicans in children with severe early childhood caries: A randomized clinical study. Journal of Indian Society of Pedodontics and Preventive Dentistry. 2016 Jan-Mar;34(1):65-70. (DOI: 10.4103/0970-4388.175518) (PMID)